

This discussion paper is/has been under review for the journal Atmospheric Chemistry and Physics (ACP). Please refer to the corresponding final paper in ACP if available.

## A permanent aerosol layer in the TTL

Q. Bourgeois et al.

# A permanent aerosol layer at the tropical tropopause layer driven by the intertropical convergence zone

Q. Bourgeois<sup>1,2</sup>, I. Bey<sup>2</sup>, and P. Stier<sup>3</sup>

<sup>1</sup>Institute of Environmental Engineering, Ecole Polytechnique Fédérale de Lausanne, Lausanne, Switzerland

<sup>2</sup>Center for Climate Systems Modeling, Institute for Atmospheric and Climate Science, ETH Zürich, Zürich, Switzerland

<sup>3</sup>Atmospheric, Oceanic and Planetary Physics, Department of Physics, Univ. of Oxford, UK

Received: 6 January 2012 – Accepted: 13 January 2012 – Published: 27 January 2012

Correspondence to: Q. Bourgeois (quentin.bourgeois@env.ethz.ch)

Published by Copernicus Publications on behalf of the European Geosciences Union.

Title Page	
Abstract	Introduction
Conclusions	References
Tables	Figures
◀	▶
◀	▶
Back	Close
Full Screen / Esc	
Printer-friendly Version	
Interactive Discussion	



## Abstract

We use observations from the Cloud-Aerosol Lidar with Orthogonal Polarization (CALIOP) satellite instrument and a global aerosol-climate model to document an aerosol layer that forms in the vicinity of the tropical tropopause layer (TTL) over the Southern Asian and Indian Ocean region. CALIOP observations suggest that the aerosol layer is present throughout the year and follows the migration of the Intertropical Convergence Zone (ITCZ). The layer is located at about 20° N during boreal summers and at about 15° S in boreal winters. The ECHAM5.5-HAM2 aerosol-climate model reproduces such an aerosol layer close to the TTL but overestimates the observed aerosol extinction. The mismatch between observed and simulated aerosols extinction are discussed in terms of uncertainties related to CALIOP and possible problems in the model. Sensitivity model simulations indicate that (i) sulfate particles resulting from SO<sub>2</sub> and DMS oxidation are the main contributors to the mean aerosol extinction in the layer throughout the year, and (ii) transport of sulfate precursors by convection followed by nucleation is responsible for the formation of the aerosol layer. The reflection of shortwave radiations by aerosols in the TTL may be negligible, however, cloud droplets formed by these aerosols may reflect about 6 W m<sup>-2</sup> back to space. Overall, this study provides new insights in term of composition of the tropical upper troposphere.

## 1 Introduction

Aerosols play a key role in many important aspects of the atmosphere. They influence the radiative balance of the Earth by scattering and absorbing solar radiation (the direct effect), and by modifying cloud properties (the indirect effect). They interact with gaseous species by acting as sites where heterogeneous reactions can occur, and also affect air quality and human health. In the lower troposphere, aerosols have in average a lifetime of less than a week and thus mainly impact air quality and climate on regional

ACPD

12, 2863–2889, 2012

## A permanent aerosol layer in the TTL

Q. Bourgeois et al.

Title Page

Abstract

Introduction

Conclusions

References

Tables

Figures

◀

▶

◀

▶

Back

Close

Full Screen / Esc

Printer-friendly Version

Interactive Discussion



to continental scales. However, their effects may last longer in the upper troposphere due to the absence of liquid clouds to efficiently scavenge them (Rasch et al., 2008). In addition, secondary aerosols formed by upper tropospheric nucleation source may serve as source of cloud condensation nuclei (Merikanto et al., 2009). It is thus crucial to assess the distribution of aerosols in the upper part of the troposphere where they can remain longer and affect climate.

While few aerosol observations are available in the upper troposphere in comparison with surface sites, there are indications that aerosol loadings above 10 km are far from being negligible, and high numbers of nucleation particles are frequently found in the free troposphere (Twohy et al., 2002; Kulmala and Kerminen, 2008). For example, Clarke and Kapustin (2002) collected in situ measurements in the tropical free troposphere over the Pacific and observed very low aerosol mass but very high number concentrations between 10 and 12 km (e.g., about  $18\,000\text{ cm}^{-3}$  at 11 km in the Pacific). They indicated that these aerosols are mainly sulfate particles in the nucleation mode. Weigel et al. (2011) recently reported in situ measurements of newly formed particles at about 1–4 km below the tropical tropopause layer (i.e., at an altitude of about 12–15 km). According to their measurements, 75 to 90 % of these aerosols are volatile, which is an indication that they could be sulfate aerosols. Froyd et al. (2009) reported that about 80 % of observed particles between 12 and 19 km in the tropical Pacific are sulfate-organic aerosols.

Vernier et al. (2011a) recently used scattering ratio from the CALIOP instrument to document an aerosol layer forming between 13 and 18 km during summer over Asia ( $15\text{--}45^\circ\text{ N}$ ,  $5\text{--}105^\circ\text{ E}$ ). Vernier et al. (2011a) argued that the observed scattering ratio is probably attributable to aerosol and not ice clouds due to different optical properties. However, the origins and the aerosol composition of this layer remain unknown.

In this study, we build on the work of Vernier et al. (2011a) and use the CALIOP data to demonstrate that an aerosol layer resides in the TTL throughout the year and follows the seasonal migration of the ITCZ (Sect. 2.1). We further characterize the layer using the global aerosol-climate ECHAM5.5-HAM2 model (Sect. 2.2). In Sect. 3, we discuss

## A permanent aerosol layer in the TTL

Q. Bourgeois et al.

Title Page

Abstract

Introduction

Conclusions

References

Tables

Figures

◀

▶

◀

▶

Back

Close

Full Screen / Esc

Printer-friendly Version

Interactive Discussion



possible uncertainties and problems related to both the model and the observations, in an attempt to reconcile the two. Conclusions and perspectives are given in Sect. 4.

## 2 A permanent aerosol layer at the tropical tropopause layer

### 2.1 CALIOP observations

5 The CALIOP instrument on-board the Cloud-Aerosol Lidar and Infrared Pathfinder Satellite Observation (CALIPSO) satellite (Winker et al., 2007, 2009) is suitable for the detection of aerosols in the atmosphere. In particular, CALIOP is dedicated to the retrieval of aerosol vertical distributions in the troposphere and the lower stratosphere. In this study, we use the standard CALIPSO 5 km Aerosol and Cloud Layer Version  
10 3 products from January 2007 to December 2009 (Hu et al., 2009; Liu et al., 2009; Omar et al., 2009; Winker et al., 2009; Young and Vaughan, 2009). Aerosol extinction and aerosol optical depth (AOD) are retrieved at 532 nm. CALIOP uncertainties are discussed in Sect. 3.

15 Building upon the work of Vernier et al. (2011a), we performed a detailed examination of the CALIOP products in the troposphere over a region covering a large fraction of the Asian continent and Indian Ocean (extending from 20° S to 30° N and from 5 to 105° E). We constructed a timeseries of CALIOP daily mean aerosol extinction over this region from January 2007 to December 2009 (top panel in Fig. 1) by averaging the vertical daily mean aerosol extinctions of all orbit tracks passing through the region  
20 defined before. As expected, aerosol extinctions are larger in the lower troposphere, close to pollution sources. The seasonal cycle in aerosol extinction in the lower troposphere is similar throughout the 3 yr. An aerosol layer of about 2 km depth is seen at an altitude from 16 to 18 km during the 3 yr of observations. During summer, this very likely corresponds to the aerosol layer described in Vernier et al. (2011a), but  
25 we find that the layer remains throughout the winters if one considers a region that includes the seasonal migration of the ITCZ, extending from 20° S to 30° N (note that

## A permanent aerosol layer in the TTL

Q. Bourgeois et al.

Title Page

Abstract

Introduction

Conclusions

References

Tables

Figures

◀

▶

◀

▶

Back

Close

Full Screen / Esc

Printer-friendly Version

Interactive Discussion



## A permanent aerosol layer in the TTL

Q. Bourgeois et al.

Title Page

Abstract

Introduction

Conclusions

References

Tables

Figures

◀

▶

◀

▶

Back

Close

Full Screen / Esc

Printer-friendly Version

Interactive Discussion



Vernier et al. (2011a) used a region extending from 15 to 45° N). Figure 2 depicts a latitudinal plot of aerosol extinction sampled at the altitude of 16–18 km that shows that the aerosol layer moves northward or southward according to the season. In particular, the aerosol layer migrates from 20° S in boreal winter to 30° N in boreal summer and matches very well the location of the ITCZ (not shown). This suggests that aerosol precursors and/or aerosols could be transported to the TTL through deep convection associated with the ITCZ (see Sect. 2.2.2 for more details). Once aerosols reach the TTL, their lifetime is likely to increase substantially as hardly any little scavenging can take place due to little concentrations of ice crystals and no liquid phase clouds. Rasch et al. (2008) show that sulfate aerosols during a volcanic period have a lifetime of about 2 yr above the tropopause and are likely only removed by sedimentation as ice crystals are inefficient at removing aerosols (Henning et al., 2004).

In the next section, we compare the CALIOP observations with results from the global aerosol-climate ECHAM5.5-HAM2 model and characterize the aerosol layer using a series of model sensitivity simulations.

## 2.2 ECHAM5.5-HAM2 model results

### 2.2.1 Brief model description

The ECHAM5 (Roeckner et al., 2003) general circulation model (GCM) is coupled with the aerosol module HAM (Stier et al., 2005), here employed in its version ECHAM5.5-HAM2 (Zhang et al., 2012). The aerosol module HAM2 predicts the size distribution and composition (mixing state) of aerosols including sulfate, black carbon (BC), organic carbon (OC), dust and sea salt. The particle size distribution is described by 7 lognormal modes (Vignati et al., 2004) including a sulfate only nucleation mode, three internally mixed hydrophilic modes (Aitken, accumulation and coarse) containing all species, an internally mixed hydrophobic BC/OC mode (Aitken) and two externally mixed dust modes (accumulation and coarse). Nucleation is estimated as a function of temperature, relative humidity, gas phase sulfuric acid concentration, gas

phase sulfuric acid condensation sink and ionization rate following the scheme of Kazil and Lovejoy (2007) and implemented in ECHAM5.5-HAM2 as described in Kazil et al. (2010). Integration of the time evolution equation for gas phase  $\text{H}_2\text{SO}_4$  including chemical production, nucleation and condensation is performed as described in Kokkola et al. (2009). Processes of coagulation and sulfuric acid condensation occur in and/or in between aerosol modes allowing particles to grow and to move from one mode to another (Stier et al., 2005). In the model, OC only originates from primary emissions (i.e. without an explicit secondary organic aerosol scheme) which may result in an underestimate of OC (Kazil et al., 2010). An explicit below-cloud scavenging (Croft et al., 2009) and a semi empirical water uptake schemes were implemented. A double-moment cloud microphysics scheme including prognostic equations for number concentrations of liquid droplets and ice crystals is used (Lin and Leaitch, 1997; Lohmann et al., 1999, 2007, 2008). The in-cloud scavenging scheme makes use of scavenging ratios that are prescribed as a function of aerosol size, aerosol mixing state and cloud type (Stier et al., 2005). In the simulations described in this paper, aerosol scavenging parameters were modified following recommendations from Bourgeois and Bey (2011).

ECMWF meteorological fields (ERA-INTERIM) were used to nudge the model enabling the representation of large-scale weather systems for specific years. Anthropogenic emissions for aerosols are prescribed using the ARCTAS inventory, which is representative of the year 2008 (<http://www.cgrer.uiowa.edu/arctas/emission.html>). A mix of FLAMBE (Reid et al., 2009) and GFEDv3 (van der Werf et al., 2010) inventories were used for biomass burning emissions as reported in Bourgeois and Bey (2011). A 3-year simulation was performed at a T63L31 resolution (about  $1.9 \times 1.9^\circ$  in the horizontal dimension and 31 vertical levels from the surface up to 10 hPa). Aerosol extinction and AOD are reported at 550 nm.

## 2.2.2 Comparison with CALIOP

The model is sampled along CALIOP orbits passing through the chosen region. Figure 1 (middle panel) shows the aerosol extinction timeseries simulated by the model

## A permanent aerosol layer in the TTL

Q. Bourgeois et al.

Title Page

Abstract

Introduction

Conclusions

References

Tables

Figures

◀

▶

◀

▶

Back

Close

Full Screen / Esc

Printer-friendly Version

Interactive Discussion



for the same region and time period than those provided by CALIOP while Fig. 3 compares the observed and simulated annual mean vertical distribution of aerosol extinctions over our region of interest. The model reproduces well aerosol extinctions from the surface to about 8 km but the discrepancy is rather large above 8 km although both the model and the observations similarly show the presence of an enhanced aerosol layer in the TTL (at about 16 km). Observed aerosol extinctions sharply decrease between 8 and 15 km while simulated aerosol extinctions remain at a similar value from 8 to 11 km and slightly increase from 11 to 16 km. In both the observations and the model results, aerosol extinction maximizes at around 16 km, where the model simulates the mean tropopause height for the chosen region. The altitude of the observed and simulated aerosol extinction maxima are similar but the model simulates a much broader aerosol layer than the CALIOP retrieval, which shows a finer aerosol layer of about 2 km thick. The magnitude of these aerosol enhancements are also different with a mean aerosol extinction of  $2 \cdot 10^{-4}$  and  $7 \cdot 10^{-4} \text{ km}^{-1}$  in the observation and the model, respectively. The simulated and observed monthly mean AOD integrated throughout the troposphere show overall good agreement ( $R^2 = 0.64$ ), but this good agreement reflects the fact that the total AOD is largely influenced by the high amount of aerosols found in the planetary boundary layer.

### 2.2.3 Characterization of the simulated aerosol layer

In the following we discuss the monthly mean aerosol extinctions of the aerosol layer for the different aerosol species and modes simulated in the model (approximated by volume weighted average of the refractive indices of the individual species). According to the model, sulfate, water and OC contribute 53, 29, and 11 %, respectively, to the aerosol layer extinction, while dust, sea salt, and BC contribute 7 % in total (Fig. 4). The sulfate contribution in the aerosol layer is higher during summer, which likely reflects the ITCZ located over South East Asia where large amounts of anthropogenic  $\text{SO}_2$  (sulfate precursor) are emitted. OC and BC contribute more in winter than in summer to the aerosol layer because biomass burning emissions are large during boreal winter

## A permanent aerosol layer in the TTL

Q. Bourgeois et al.

Title Page

Abstract

Introduction

Conclusions

References

Tables

Figures

◀

▶

◀

▶

Back

Close

Full Screen / Esc

Printer-friendly Version

Interactive Discussion



in Southeast Asia (van der Werf et al., 2010). The dust signature is maximum from April to July (about 5 %) and is likely related to dust storms occurring over the Thar desert in Western India during the pre-monsoon season (Dey et al., 2004). The simulated lifetimes of sulfate and OC in the aerosol layer with respect to wet deposition and sedimentation are 116 and 215 days, respectively. Sedimentation contributes 89 and 79 % to the sulfate and OC removal, respectively. The remaining 11 and 21 % are due to in-cloud aerosol scavenging.

The annual mean aerosol extinction between 16 and 17.5 km (i.e. at the maximum aerosol extinction) is dominated at 91 % by internally-mixed aerosols in the accumulation mode. The internally-mixed coarse mode contributes 8 % and the remaining 1 % is due to other modes such as internally-mixed Aitken mode and externally-mixed modes. In terms of aerosol number concentration, the nucleation mode contributes 99.5 %. This indicates that 0.5 % of the aerosol number concentration (other than aerosols in the nucleation mode) contributes 99 % of the aerosol extinction (91 and 8 % from the internally-mixed accumulation and coarse mode, respectively).

Figure 5 shows the vertical profile of aerosol number concentrations in the nucleation mode. The maximum aerosol number concentration occurs just below the tropopause from 14 to 16 km. The annual mean aerosol number concentration for nucleated aerosols larger than 3 nm ( $D_p > 3$  nm) in this layer is about  $45\,000\text{ cm}^{-3}$  (at STP). The nucleation aerosol layer between 14 and 16 km is not visible in Fig. 1 because aerosols below 100 nm are not optically active. In order to assess the role of nucleation on the aerosol layer in the TTL, we performed a sensitivity simulation in which nucleation was turned off. We find that the aerosol number concentration decreases while the mean aerosol extinction of the aerosol layer increases by about 10 % when nucleation is turned off. This likely reflects the fact that without nucleation, sulfate in the gas phase can only condense on pre-existing particles and do not form new particles. This allows aerosols to grow into a radiatively active size range. We find that 60 % of particles in the accumulation mode in the aerosol layer are formed by nucleation. Hence, nucleation is a significant process in the formation of the aerosol layer in the TTL. We also

**A permanent aerosol layer in the TTL**

Q. Bourgeois et al.

Title Page

Abstract

Introduction

Conclusions

References

Tables

Figures

◀

▶

◀

▶

Back

Close

Full Screen / Esc

Printer-friendly Version

Interactive Discussion



performed a series of sensitivity simulations in which anthropogenic, biomass burning, volcanic and DMS emissions were turned off and estimated the relative contributions of these different emissions by subtracting results from the sensitivity simulations to those from the reference one. These simulations (Fig. 6) show that sulfate in the aerosol layer is predominantly from SO<sub>2</sub> and DMS sources. SO<sub>2</sub> anthropogenic and volcanic emissions account for 35 % each of the total sulfate extinction, SO<sub>2</sub> biomass burning emissions account for 5 %, and DMS terrestrial and marine emissions account for 25 %. Thus, 65 and 35 % of the total sulfate extinction are due to natural and anthropogenic sources, respectively.

In Sect. 2.1, we hypothesis (as many other studies investigating aerosol distribution in the upper troposphere) that the formation of the TTL aerosol layer is at least to some extent driven by deep convection associated with the ITCZ. In the tropics, Hadley cells largely dominate air circulation. Surface air masses from the Southern and Northern Hemisphere converge at the ITCZ near the equator. They rise toward the tropopause near the equator, move slowly poleward, descend toward the surface in the subtropics, and flow back toward the Equator near the surface. Over the Asian region, the ITCZ is located between 5 and 15° S in boreal winter and between 5 and 30° N in boreal summer (Chao, 2000; Lawrence and Lelieveld, 2010). In boreal summer, the ITCZ is located over India (Asian monsoon) where vigorous deep convection reaching across the tropopause and up to the lower stratosphere can take place (Gadgil, 2003). Fueglistaler et al. (2009) shows that during deep convection event, the main outflow can reach 200 hPa (about 12.5 km near the equator) with rare penetration of the outflow in the TTL. Liu and Zipser (2005) estimated that 1.3 % of the convective air masses reach 14 km and only 0.1 % of them penetrate into the TTL. In a sensitivity simulation in which tracers (including aerosol precursors and aerosols) did not experience convection (i.e. do not undergo convective transport), the aerosol layer does not form (Fig. 6), which supports the conclusion that convection associated with the ITCZ is directly responsible for the formation of the TTL aerosol layer.

## A permanent aerosol layer in the TTL

Q. Bourgeois et al.

[Title Page](#)[Abstract](#)[Introduction](#)[Conclusions](#)[References](#)[Tables](#)[Figures](#)[◀](#)[▶](#)[◀](#)[▶](#)[Back](#)[Close](#)[Full Screen / Esc](#)[Printer-friendly Version](#)[Interactive Discussion](#)

### 3 Discussion

While observed and simulated aerosol extinctions agree quite well in the lower troposphere, there are significant differences in the upper troposphere. In the following we discuss possible reasons related to both the model and the observations for these differences. Several studies have reported that uncertainties of CALIOP extinction and AOD are likely to be large. For example, a case study reported by Kacenelenbogen et al. (2011) shows that CALIOP version 3 AOD is a factor of two lower than MODIS and AERONET observations in North America. Yu et al. (2010) also reported that CALIOP AOD observations for different geopolitical regions are lower than MODIS AOD observations. CALIOP uncertainties are associated with the sensitivity of the instrument, the misclassification of aerosols and clouds, and the determination of the lidar ratio for each type of aerosol (Winker et al., 2009, and references hereafter).

In the particular case of very low aerosol extinctions as found in the TTL, the sensitivity threshold ( $3.10^{-4} \text{ km}^{-1} \text{ sr}^{-1}$  Winker et al., 2009) of CALIOP may be the main issue. As a result, extinctions in the aerosol layer in the TTL may be too low to be detected, and thus they may be classified as “clear air” (Winker et al., 2009). Chazette et al. (2010) suggested that the lower AOD detection limit of CALIOP is about 0.07 during night and 0.1 during day. Another study (Bourgeois and Bey, 2012) also found that CALIOP significantly underestimates low AOD values in the Northern Hemisphere, in particular below 0.1. Therefore, the sensitivity threshold on the aerosol attenuated backscatter may result in an underestimate of aerosol extinction in the upper troposphere where aerosol extinctions are particularly low. In addition, a maximum uncertainty of 30 % for aerosol extinction is associated with the determination of the lidar ratio by the CALIOP algorithm (Omar et al., 2009).

A misclassification of the aerosol type can also induce large errors on the aerosol extinction because aerosol lidar ratios range from 10 to 110 sr (Anderson et al., 2000). Oo and Holz (2011) showed that in some cases, the CALIOP version 3 algorithm misclassifies fine aerosols as coarse over oceans (i.e. the algorithm considers a lidar ratio of

## A permanent aerosol layer in the TTL

Q. Bourgeois et al.

Title Page

Abstract

Introduction

Conclusions

References

Tables

Figures

◀

▶

◀

▶

Back

Close

Full Screen / Esc

Printer-friendly Version

Interactive Discussion



**A permanent aerosol layer in the TTL**

Q. Bourgeois et al.

20 sr instead of 40 sr) inducing an underestimate of the AOD by about a factor of 2. Another source of uncertainty is associated with the cloud-aerosol discrimination (CAD) which is characterized by a confidence value (Liu et al., 2009). Di Pierro et al. (2011) used CALIOP version 2 products and show that dust aerosol can be misclassified as clouds due to their high depolarization ratio. However, Redemann et al. (2011) reported that CALIOP version 3 AOD are similar to or better agree with MODIS observations over oceans than the previous version. Redemann et al. (2011) and Yu et al. (2010) showed that CALIOP observations better reproduce MODIS observations when they used a filter for CALIOP data. For example, Yu et al. (2010) used only “cloud-free” profiles and aerosol data with a CAD score between  $-50$  and  $-100$  corresponding to a confidence in aerosol data higher than 50%. In contrast, no screening using CAD was used in this study because the CAD score of the aerosol layer is between  $-50$  and 0 (not shown), which corresponds to a confidence in aerosol classification lower than 50%. The low CAD confidence is likely due to the fact that retrieved extinctions in the aerosol layer are very low (close to the detection limit of the instrument).

A recent study suggested that overshooting of clean air during convective processes cleans the upper tropical troposphere and lower stratosphere (between 14 and 20 km) in the southern tropic convective season (Vernier et al., 2011b), which is in apparent contradiction with our results. Vernier et al. (2011b) used a similar version of CALIOP product than in our study but applied different averaging or correction on the data as described in Vernier et al. (2009): First, they averaged nighttime extinctions over large boxes ( $2^\circ$  longitude  $\times$   $1^\circ$  latitude  $\times$  200 m in vertical); Second, they process CALIOP data by using a 36–39 km range for the free aerosol background instead of 30–34 km in the CALIOP algorithm; Third, they removed aerosol extinction measurements with depolarization ratios larger than 0.05 to avoid a possible misclassification of ice crystals in aerosols. We argue, however, that averaging CALIOP data over large grid cells as used in Vernier et al. (2009) (rather than making use of the fine CALIOP resolution) suppresses the aerosol layer in the TTL (not shown). Omar et al. (2009) and Hu et al. (2009) reported that aerosol and ice cloud depolarization ratios typically range

[Title Page](#)[Abstract](#)[Introduction](#)[Conclusions](#)[References](#)[Tables](#)[Figures](#)[◀](#)[▶](#)[◀](#)[▶](#)[Back](#)[Close](#)[Full Screen / Esc](#)[Printer-friendly Version](#)[Interactive Discussion](#)

from 0 to 0.05 and from 0.25 to 0.54, respectively. Therefore, averaging high depolarization ratios of ice clouds (0.25 to 0.54) with low depolarization ratios of aerosols (0 to 0.05) over large grid cells results in depolarization ratios larger than 0.05, which artificially “remove” aerosol layers with weak depolarization ratios from the dataset. This is likely to happen because aerosols and clouds cohabite at the TTL, which makes their distinction difficult. For example, Weigel et al. (2011) observed that aerosols and ice clouds coexist below the TTL in agreement with Thomas et al. (2002) who reported measurements of cirrus clouds there as well. As a matter of fact, the model also simulates a layer of ice crystals between 10 and 16 km just below the aerosol layer (not shown), which possibly confirms the co-existence of aerosols and ice crystals in the TTL. To test the implications of applying a screening based on depolarization ratios on our result, we removed aerosol extinctions with depolarization ratios larger than 0.05 for all profiles above our region of interest but without averaging observations over large grid cells (Fig. 3). This screening results in a decrease of the aerosol extinctions throughout the column but the large aerosol extinctions in the PBL as well as the aerosol enhancement around the TTL remain clearly visible.

Sensitivity model simulations provide additional evidence that the TTL layer is likely composed of aerosols. Two main discrepancies are however remarkable between the model and the observations. First, the aerosol layer in the model is thicker than in the observations, which may be related to the quite large vertical resolution of the model at this altitude (about 1.4 km). Second, aerosol extinctions in the TTL are larger in the model than in the observations which may indicate issues related to sulfate formation, removal or convection in the model. To our knowledge, no measurements of the total number of nucleated particles are available at these altitudes due to extreme meteorological conditions. Clarke and Kapustin (2002) report a maximum aerosol number concentration of  $19\,000\text{ cm}^{-3}$  ( $D_p > 3\text{ nm}$ ) at 11 km in the Pacific tropical region and a concentration of about  $7\,000\text{ cm}^{-3}$  ( $D_p > 3\text{ nm}$ ) at 12 km. The simulated annual mean aerosol number concentration at 11 km in the tropical Pacific region is about  $45\,000\text{ cm}^{-3}$  ( $D_p > 3\text{ nm}$ ), indicating that the model overestimates observed values.

## A permanent aerosol layer in the TTL

Q. Bourgeois et al.

[Title Page](#)[Abstract](#)[Introduction](#)[Conclusions](#)[References](#)[Tables](#)[Figures](#)[◀](#)[▶](#)[◀](#)[▶](#)[Back](#)[Close](#)[Full Screen / Esc](#)[Printer-friendly Version](#)[Interactive Discussion](#)

This overestimate was previously reported in Kazil et al. (2010), who suggested that this was not due to a nucleation processes. In addition, the simulated maximum of nucleated aerosol number concentration is located between 14 and 16 km, i.e. higher than the altitude suggested by observations (11 km, even though observations stop at 12 km, Clarke and Kapustin, 2002). This may indicate a too strong convective transport of aerosols and/or aerosol precursors in that region.

SO<sub>2</sub> Asian anthropogenic emissions could be also too large in our model though our global and Asian anthropogenic emissions of SO<sub>2</sub> (110 and 40 Tg yr<sup>-1</sup>, respectively) agree well with recent estimates such as those provided in Lee et al. (2011). The missing “connection” in CALIOP between aerosols in the lower troposphere and the TTL (Figs. 1 and 3), also discussed in Vernier et al. (2011a), likely results from the presence of convective clouds that mask vertical transport of aerosols. The model actually simulates large export of sulfate precursors (i.e. SO<sub>2</sub> and DMS) toward the tropical upper troposphere associated with convective processes. These gases further oxidize and their product nucleates to form new particles (e.g., the nucleation aerosol layer between 13 and 16 km) or condensate on pre-existing particles, inducing aerosol growth. These particles reach a critical size that matters for extinction once they are in the TTL. This likely explains why no “connection” is seen between the lower troposphere and the upper troposphere in CALIOP.

From these different elements, we conclude that the presence of an aerosol layer in the TTL with a substantial contribution from anthropogenic activities is very likely, even though the amount of aerosols in the TTL aerosol layer is still uncertain.

## 4 Conclusions and perspectives

CALIOP observations indicate that an aerosol layer remains the entire year in the TTL (at about 16–18 km) and follows the migration of the ITCZ. The confidence for the aerosol-cloud discrimination in the CALIOP retrieval algorithm is relatively low (lower than 50 %), likely because aerosol extinctions in this layer are close to the detection

## A permanent aerosol layer in the TTL

Q. Bourgeois et al.

Title Page

Abstract

Introduction

Conclusions

References

Tables

Figures

◀

▶

◀

▶

Back

Close

Full Screen / Esc

Printer-friendly Version

Interactive Discussion



limit of the instrument. However, particulate depolarization ratios of the particles in the layer are mostly lower than 0.05, which is a typical value for aerosols other than dust.

In order to characterize this aerosol layer, we used the ECHAM5.5-HAM2 model. The model simulates an aerosol layer during the whole year and at the same altitude but the magnitude of the aerosol layer extinction is substantially larger in the model than in observations and the seasonal cycle of the layer is stronger in the model. A sensitivity simulation shows that convection is unambiguously responsible for the formation of the simulated aerosol layer in the TTL. According to the model, sulfate, water and OC contribute 53, 29, and 11 %, respectively, to the aerosol layer extinction, while dust, sea salt, and BC contribute 7 % in total. Extinction due to sulfate aerosols comes from the nucleation and condensation of sulfuric acid, which, in turn, comes at 75 % and 25 % from the SO<sub>2</sub> and DMS oxidation, respectively. SO<sub>2</sub> emitted by volcanic and anthropogenic emissions contributes 35 % each to the sulfate extinction in the aerosol layer while DMS emitted by terrestrial biogenic and marine contributes 25 %. SO<sub>2</sub> emitted in biomass burning emissions contribute 5 %. Therefore, 35 % of the extinction in term of sulfate in the aerosol layer are related to anthropogenic activities while 65 % are due to natural sources. The fast increase in anthropogenic pollution sources in Asia may further increase the proportion due to human activities and, as such, the total aerosol extinction of the TTL aerosol layer, with some possible implications for the chemical and radiative impacts of this aerosol layer. The aerosol layer may have substantial effects. As it is mostly composed of sulfate and sulfate aerosols that reflect sunlight, it likely decreases solar radiations absorbed by the atmosphere and induces a cooling of the troposphere over the Southern Asian region. The AOD of the TTL aerosol layer accounts for less than 1 % of the AOD integrated throughout the troposphere (from the surface to 20 km), and therefore the direct effect of aerosols on solar radiation is probably small. However, aerosols can act as CCN and form cloud droplets that also reflect solar radiation. For example, Merikanto et al. (2009) reported that secondary aerosols derived from upper tropospheric nucleation contributes 14 % of CCN at 0.2 % supersaturation in Southeast Asian low level clouds. Over our region of interest, the

## A permanent aerosol layer in the TTL

Q. Bourgeois et al.

Title Page

Abstract

Introduction

Conclusions

References

Tables

Figures

◀

▶

◀

▶

Back

Close

Full Screen / Esc

Printer-friendly Version

Interactive Discussion



model indicates that 29 and  $42 \text{ W m}^{-2}$  are reflected back to space by aerosols and clouds, respectively, in the shortwave radiation. Hence, about  $6 \text{ W m}^{-2}$  (i.e. 14 % of  $42 \text{ W m}^{-2}$ ) are reflected back to space due the cloud formation by aerosols in the TTL. From a chemical point of view, sulfate may reduce ozone production in the TTL and in the stratosphere by reacting with ozone precursors (Unger et al., 2006).

Effects of aerosols, especially sulfate particles, in the TTL have been carefully studied for geoengineering purposes (e.g., Wigley, 2006; Rasch et al., 2008). Some scientists and non-scientists proposed to inject sulfate aerosols in the stratosphere to counter global warming associated with increasing greenhouse gases concentrations. However, impacts are still uncertain and more comprehensive studies are needed before any definitive conclusion can be reached and the impacts of such propositions assessed. The semi-natural aerosol layer over Southeast Asia and the Indian Ocean described in this study provides great opportunity for better understanding and assessing the chemical and radiative impacts of sulfate aerosols in the upper troposphere. Further characterization and investigation of the TTL aerosol layer are therefore needed to reduce remaining uncertainties, especially those related to lidar ratio assignment, cloud aerosol discrimination and measurement threshold of the aerosol attenuated backscatter in CALIOP, and to convection strength, and aerosol formation and deposition in the model.

*Acknowledgements.* This work was supported by funding from the Swiss National Science Foundation under the grant 200020-124928 and contributes to the EU FP7 IP PEGASOS (FP7-ENV-2010/265148). We thank G. Frontoso, S. Rast and S. Ferrachat for their help with the ECHAM5-HAM code. We acknowledge the CALIOP team for acquiring and processing data as well as the ICARE team for providing and maintaining the computational facilities to store and treat them.

## References

Anderson, T. L., Masonis, S. J., Covert, D. S., Charlson, R. J., and Rood, M. J.: In situ measurement of the aerosol extinction-to-backscatter ratio at a polluted continental site, J. Geophys.

## A permanent aerosol layer in the TTL

Q. Bourgeois et al.

Title Page

Abstract

Introduction

Conclusions

References

Tables

Figures

◀

▶

◀

▶

Back

Close

Full Screen / Esc

Printer-friendly Version

Interactive Discussion



**A permanent aerosol layer in the TTL**

Q. Bourgeois et al.

Title Page

Abstract

Introduction

Conclusions

References

Tables

Figures

◀

▶

◀

▶

Back

Close

Full Screen / Esc

Printer-friendly Version

Interactive Discussion



- Res., 105, 26907–26915, 2000. 2872
- Bourgeois, Q. and Bey, I.: Pollution transport efficiency toward the Arctic: sensitivity to aerosol scavenging and source regions, *J. Geophys. Res.*, 116, D08213, doi:10.1029/2010JD015096, 2011. 2868
- 5 Bourgeois, Q. and Bey, I.: Aerosol interannual variability: assessment of AOD retrievals from CALIOP and model comparison, in preparation, 2012. 2872
- Chao, W. C.: Multiple quasi equilibria of the ITCZ and the origin of monsoon onset, *J. Atmos. Sci.*, 57, 641–651, 2000. 2871
- Chazette, P., Raut, J.-C., Dulac, F., Berthier, S., Kim, S.-W., Royer, P., Sanak, J., Loaëc, S., and Grigaut-Desbrosses, H.: Simultaneous observations of lower tropospheric continental aerosols with a ground-based, an airborne, and the spaceborne CALIOP lidar system, *J. Geophys. Res.*, 115, D00H31, doi:10.1029/2009JD012341, 2010. 2872
- 10 Clarke, A. D. and Kapustin, V. N.: A pacific aerosol survey. Part I: A decade of data on particle production, transport, evolution, and mixing in the troposphere, *J. Atmos. Sci.*, 59, 363–382, 2002. 2865, 2874, 2875
- 15 Croft, B., Lohmann, U., Martin, R. V., Stier, P., Wurzler, S., Feichter, J., Posselt, R., and Ferrachat, S.: Aerosol size-dependent below-cloud scavenging by rain and snow in the ECHAM5-HAM, *Atmos. Chem. Phys.*, 9, 4653–4675, doi:10.5194/acp-9-4653-2009, 2009. 2868
- 20 Dey, S., Tripathi, S. N., Singh, R. P., and Holben, B. N.: Influence of dust storms on the aerosol optical properties over the Indo–Gangetic Basin, *J. Geophys. Res.*, 109, D20,211, doi:10.1029/2004JD004924, 2004. 2870
- Di Pierro, M., Jaeglé, L., and Anderson, T. L.: Satellite observations of aerosol transport from East Asia to the Arctic: three case studies, *Atmos. Chem. Phys.*, 11, 2225–2243, doi:10.5194/acp-11-2225-2011, 2011. 2873
- 25 Froyd, K. D., Murphy, D. M., Sanford, T. J., Thomson, D. S., Wilson, J. C., Pfister, L., and Lait, L.: Aerosol composition of the tropical upper troposphere, *Atmos. Chem. Phys.*, 9, 4363–4385, doi:10.5194/acp-9-4363-2009, 2009. 2865
- Fueglistaler, S., Dessler, A. E., Dunkerton, T. J., Folkins, I., Fu, Q., and Mote, P. W.: Tropical tropopause layer, *Rev. Geophys.*, 47, RG1004, doi:10.1029/2008RG000267, 2009. 2871
- 30 Gadgil, S.: The Indian monsoon and its variability, *Annu. Rev. Earth Pl. Sc.*, 31, 429, 2003. 2871
- Henning, S., Bojinski, S., Diehl, K., Ghan, S., Nyeki, S., and Weingartner, E.:

**A permanent aerosol layer in the TTL**

Q. Bourgeois et al.

[Title Page](#)[Abstract](#)[Introduction](#)[Conclusions](#)[References](#)[Tables](#)[Figures](#)[◀](#)[▶](#)[◀](#)[▶](#)[Back](#)[Close](#)[Full Screen / Esc](#)[Printer-friendly Version](#)[Interactive Discussion](#)

Aerosol partitioning in natural mixed-phase clouds, *Geophys. Res. Lett.*, 31, L06,101, doi:10.1029/2003GL019025, 2004. 2867

Hu, Y., Winker, D., Vaughan, M., Lin, B., Omar, A., Trepte, C., Flittner, D., Yang, P., Nasiri, S. L., Baum, B., Sun, W., Liu, Z., Wang, Z., Young, S., Stamnes, K., Huang, J., Kuehn, R., and Holz, R.: CALIPSO/CALIOP cloud phase discrimination algorithm, *J. Atmos. Ocean. Tech.*, 26, 2293–2309, 2009. 2866, 2873

Kacenenbogen, M., Vaughan, M. A., Redemann, J., Hoff, R. M., Rogers, R. R., Ferrare, R. A., Russell, P. B., Hostetler, C. A., Hair, J. W., and Holben, B. N.: An accuracy assessment of the CALIOP/CALIPSO version 2/version 3 daytime aerosol extinction product based on a detailed multi-sensor, multi-platform case study, *Atmos. Chem. Phys.*, 11, 3981–4000, doi:10.5194/acp-11-3981-2011, 2011. 2872

Kazil, J. and Lovejoy, E. R.: A semi-analytical method for calculating rates of new sulfate aerosol formation from the gas phase, *Atmos. Chem. Phys.*, 7, 3447–3459, doi:10.5194/acp-7-3447-2007, 2007. 2868

Kazil, J., Stier, P., Zhang, K., Quaas, J., Kinne, S., O'Donnell, D., Rast, S., Esch, M., Ferrachat, S., Lohmann, U., and Feichter, J.: Aerosol nucleation and its role for clouds and Earth's radiative forcing in the aerosol-climate model ECHAM5-HAM, *Atmos. Chem. Phys.*, 10, 10733–10752, doi:10.5194/acp-10-10733-2010, 2010. 2868, 2875

Kokkola, H., Hommel, R., Kazil, J., Niemeier, U., Partanen, A.-I., Feichter, J., and Timmreck, C.: Aerosol microphysics modules in the framework of the ECHAM5 climate model – intercomparison under stratospheric conditions, *Geosci. Model Dev.*, 2, 97–112, doi:10.5194/gmd-2-97-2009, 2009. 2868

Kulmala, M. and Kerminen, V.-M.: On the formation and growth of atmospheric nanoparticles, *Atmos. Res.*, 90, 132–150, 2008. 2865

Lawrence, M. G. and Lelieveld, J.: Atmospheric pollutant outflow from southern Asia: a review, *Atmos. Chem. Phys.*, 10, 11017–11096, doi:10.5194/acp-10-11017-2010, 2010. 2871

Lee, C., Martin, R. V., van Donkelaar, A., Lee, H., Dickerson, R. R., Hains, J. C., Krotkov, N., Richter, A., Vinnikov, K., and Schwab, J. J.: SO<sub>2</sub> emissions and lifetimes: estimates from inverse modeling using in situ and global, space-based (SCIAMACHY and OMI) observations, *J. Geophys. Res.*, 116, D06,304, doi:10.1029/2010JD014758, 2011. 2875

Lin, H. and Leaitch, W. R.: Development of an in-cloud aerosol activation parameterization for climate modelling, in: *Proceedings of the WMO workshop on measurement of cloud properties for forecasts of weather, air quality and climate*, World Meteorological Organization,

**A permanent aerosol layer in the TTL**

Q. Bourgeois et al.

Title Page

Abstract

Introduction

Conclusions

References

Tables

Figures

◀

▶

◀

▶

Back

Close

Full Screen / Esc

Printer-friendly Version

Interactive Discussion



Geneva, 328–335, 1997. 2868

Liu, C. and Zipser, E. J.: Global distribution of convection penetrating the tropical tropopause, *J. Geophys. Res.*, 110, D23,104, doi:10.1029/2005JD006063, 2005. 2871

Liu, Z., Vaughan, M., Winker, D., Kittaka, C., Getzewich, B., Kuehn, R., Omar, A., Powell, K.,  
5 Trepte, C., and Hostetler, C.: The CALIPSO lidar cloud and aerosol discrimination: version  
2 algorithm and initial assessment of performance, *J. Atmos. Ocean. Tech.*, 26, 1198–1213,  
2009. 2866, 2873

Lohmann, U., Feichter, J., Chuang, C. C., and Penner, J. E.: Predicting the number of cloud  
droplets in the ECHAM GCM, *J. Geophys. Res.*, 104, 9169–9198, 1999. 2868

10 Lohmann, U., Stier, P., Hoose, C., Ferrachat, S., Kloster, S., Roeckner, E., and Zhang, J.: Cloud  
microphysics and aerosol indirect effects in the global climate model ECHAM5-HAM, *Atmos.  
Chem. Phys.*, 7, 3425–3446, doi:10.5194/acp-7-3425-2007, 2007. 2868

Lohmann, U., Spichtinger, P., Jess, S., Peter, T., and Smit, H.: Cirrus cloud formation and ice  
supersaturated regions in a global model, *Environ. Res. Lett.*, 3, 045022, doi:10.1088/1748-  
15 9326/3/4/045022, 2008. 2868

Merikanto, J., Spracklen, D. V., Mann, G. W., Pickering, S. J., and Carslaw, K. S.: Impact of  
nucleation on global CCN, *Atmos. Chem. Phys.*, 9, 8601–8616, doi:10.5194/acp-9-8601-  
2009, 2009. 2865, 2876

Omar, A., Winker, D. M., Kittaka, C., Vaughan, M. A., Liu, Z., Hu, Y., Trepte, C. R., Rogers, R. R.,  
20 Ferrare, R. A., Lee, K.-P., Kuehn, R. E., and Hostetler, C. A.: The CALIPSO automated  
aerosol classification and lidar ratio selection algorithm, *J. Atmos. Ocean. Tech.*, 26, 1994–  
2014, 2009. 2866, 2872, 2873

Oo, M. and Holz, R.: Improving the CALIOP aerosol optical depth using combined MODIS-  
CALIOP observations and CALIOP integrated attenuated total color ratio, *J. Geophys. Res.*,  
25 116, D14,201, doi:10.1029/2010JD014894, 2011. 2872

Rasch, P. J., Tilmes, S., Turco, R. P., Robock, A., Oman, L., Chen, C., Stenchikov, G. L.,  
and Garcia, R. R.: An overview of geoengineering of climate using stratospheric sulphate  
aerosols, *Phil. Trans. R. Soc. A*, 366, 4007–4037, doi:10.1098/rsta.2008.0131, 2008. 2865,  
2867, 2877

30 Redemann, J., Vaughan, M. A., Zhang, Q., Shinozuka, Y., Russell, P. B., Livingston, J. M.,  
Kacenelenbogen, M., and Remer, L. A.: The comparison of MODIS-Aqua (C5) and  
CALIOP (V2&V3) aerosol optical depth, *Atmos. Chem. Phys. Discuss.*, 11, 22987–23027,  
doi:10.5194/acpd-11-22987-2011, 2011. 2873

**A permanent aerosol layer in the TTL**

Q. Bourgeois et al.

Title Page

Abstract

Introduction

Conclusions

References

Tables

Figures

◀

▶

◀

▶

Back

Close

Full Screen / Esc

Printer-friendly Version

Interactive Discussion



- Reid, J. S., Hyer, E. J., Prins, E. M., Westphal, D. L., Zhang, J., Wang, J., Christopher, S. A., Curtis, C. A., Schmidt, C. C., Eleuterio, D. P., Richardson, K. A., and Hoffman, J. P.: Global monitoring and forecasting of biomass-burning smoke: description of and lessons from the fire locating and modeling of burning emissions (FLAMBE) program, *IEEE J. Sel. Top. Appl.*, 2, 144–162, 2009. 2868
- 5 Roeckner, E., Bäuml, E., Bonaventura, G., Brokopf, L., Esch, R., Giorgetta, M., Hagemann, M., Kirchner, S., Kornblueh, I., Manzini, L., Rhodin, E., Schlese, A., Schulzweida, U., and Tompkins, U.: The Atmospheric General Circulation Model ECHAM5: Part 1, Tech. Rep. 349, Max Planck Institute for Meteorology, Hamburg, Germany, 2003. 2867
- 10 Stier, P., Feichter, J., Kinne, S., Kloster, S., Vignati, E., Wilson, J., Ganzeveld, L., Tegen, I., Werner, M., Balkanski, Y., Schulz, M., Boucher, O., Minikin, A., and Petzold, A.: The aerosol-climate model ECHAM5-HAM, *Atmos. Chem. Phys.*, 5, 1125–1156, doi:10.5194/acp-5-1125-2005, 2005. 2867, 2868
- 15 Thomas, A., Borrmann, S., Kiemle, C., Cairo, F., Volk, M., Beuermann, J., Lepuchov, B., Santacesaria, V., Matthey, R., Rudakov, V., Yushkov, V., MacKenzie, A. R., and Stefanutti, L.: In situ measurements of background aerosol and subvisible cirrus in the tropical tropopause region, *J. Geophys. Res.*, 107, 4763, doi:10.1029/2001JD001385, 2002. 2874
- Twohy, C. H., Clement, C. F., Gandrud, B. W., Weinheimer, A. J., Campos, T. L., Baumgardner, D., Brune, W. H., Faloon, I., Sachse, G. W., Vay, S. A., and Tan, D.: Deep convection as a source of new particles in the midlatitude upper troposphere, *J. Geophys. Res.*, 107, 4560, doi:10.1029/2001JD000323, 2002. 2865
- 20 Unger, N., Shindell, D. T., Koch, D. M., Amann, M., Cofala, J., and Streets, D. G.: Influences of man-made emissions and climate changes on tropospheric ozone, methane, and sulfate at 2030 from a broad range of possible futures, *J. Geophys. Res.*, 111, D12,313, doi:10.1029/2005JD006518, 2006. 2877
- 25 van der Werf, G. R., Randerson, J. T., Giglio, L., Collatz, G. J., Mu, M., Kasibhatla, P. S., Morton, D. C., DeFries, R. S., Jin, Y., and van Leeuwen, T. T.: Global fire emissions and the contribution of deforestation, savanna, forest, agricultural, and peat fires (1997–2009), *Atmos. Chem. Phys.*, 10, 11707–11735, doi:10.5194/acp-10-11707-2010, 2010. 2868, 2870
- 30 Vernier, J.-P., Pommereau, J. P., Garnier, A., Pelon, J., Larsen, N., Nielsen, J., Christensen, T., Cairo, F., Thomason, L. W., Leblanc, T., and McDermid, I. S.: Tropical stratospheric aerosol layer from CALIPSO lidar observations, *J. Geophys. Res.*, 114, D00H10, doi:10.1029/2009JD011946, 2009. 2873

- Vernier, J., Thomason, L. W., and Kar, J.: Calipso detection of an asian tropopause aerosol layer, *Geophys. Res. Lett.*, 38, L07,804, doi:10.1029/2010GL046614, 2011a. 2865, 2866, 2867, 2875
- Vernier, J.-P., Pommereau, J.-P., Thomason, L. W., Pelon, J., Garnier, A., Deshler, T., Jumelet, J., and Nielsen, J. K.: Overshooting of clean tropospheric air in the tropical lower stratosphere as seen by the CALIPSO lidar, *Atmos. Chem. Phys.*, 11, 9683–9696, doi:10.5194/acp-11-9683-2011, 2011b. 2873
- Vignati, E., Wilson, J., and Stier, P.: M7: an efficient size-resolved aerosol microphysics module for large-scale aerosol transport models, *J. Geophys. Res.*, 109, D22,202, doi:10.1029/2003JD004485, 2004. 2867
- Weigel, R., Borrmann, S., Kazil, J., Minikin, A., Stohl, A., Wilson, J. C., Reeves, J. M., Kunkel, D., de Reus, M., Frey, W., Lovejoy, E. R., Volk, C. M., Viciani, S., D'Amato, F., Schiller, C., Peter, T., Schlager, H., Cairo, F., Law, K. S., Shur, G. N., Belyaev, G. V., and Curtius, J.: In situ observations of new particle formation in the tropical upper troposphere: the role of clouds and the nucleation mechanism, *Atmos. Chem. Phys.*, 11, 9983–10010, doi:10.5194/acp-11-9983-2011, 2011. 2865, 2874
- Wigley, T. M.: A combined mitigation/geoengineering approach to climate stabilization, *Science*, 314, 452–454, 2006. 2877
- Winker, D. M., Hunt, W. H., and McGill, M. J.: Initial performance assessment of CALIOP, *Geophys. Res. Lett.*, 34, L19,803, doi:10.1029/2007GL030135, 2007. 2866
- Winker, D. M., Vaughan, M. A., Omar, A., Hu, Y., Powell, K. A., Liu, Z., Hunt, W. H., and Young, S. A.: Overview of the CALIPSO mission and CALIOP data processing algorithms, *J. Atmos. Ocean. Tech.*, 26, 2310–2323, 2009. 2866, 2872
- Young, A. and Vaughan, M. A.: The retrieval of profiles of particulate extinction from cloud-aerosol lidar infrared pathfinder satellite observations (calipso) data: algorithm description, *J. Atmos. Ocean. Tech.*, 26, 1105–1119, 2009. 2866
- Yu, H., Chin, M., Winker, D. M., Omar, A. H., Liu, Z., Kittaka, C., and Diehl, T.: Global view of aerosol vertical distributions from CALIPSO lidar measurements and GOCART simulations: regional and seasonal variations, *J. Geophys. Res.*, 115, D00H30, doi:10.1029/2009JD013364, 2010. 2872, 2873
- Zhang, K., O'Donnell, D., Kazil, J., Feichter, J., Stier, P., Kinne, S., Lohmann, U., Ferrachat, S., Croft, B., Quass, J., Wan, H., Rast, S., and Esch, M.: The global aerosol-climate model ECHAM5-HAM, version 2: model evaluation and sensitivity tests, in preparation, 2012. 2867

**A permanent aerosol layer in the TTL**

Q. Bourgeois et al.

[Title Page](#)[Abstract](#)[Introduction](#)[Conclusions](#)[References](#)[Tables](#)[Figures](#)[◀](#)[▶](#)[◀](#)[▶](#)[Back](#)[Close](#)[Full Screen / Esc](#)[Printer-friendly Version](#)[Interactive Discussion](#)

## A permanent aerosol layer in the TTL

Q. Bourgeois et al.

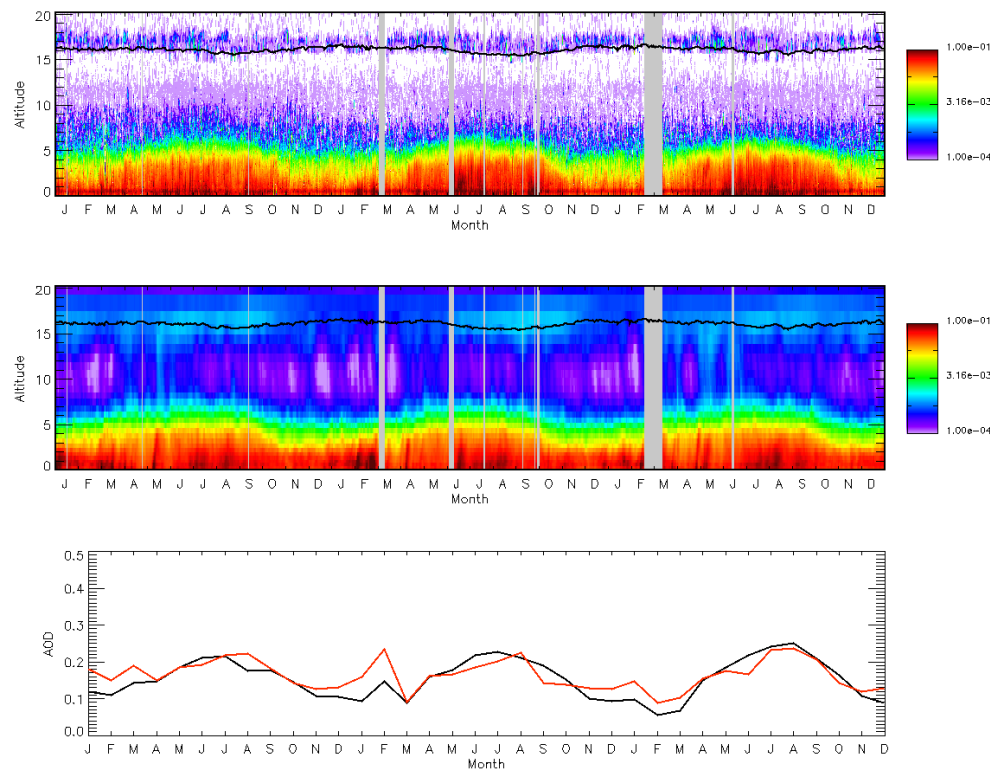


**Fig. 1.** Daily mean vertical aerosol extinctions ( $\text{km}^{-1}$ ) from January 2007 to December 2009 for the CALIOP instrument (top) and the model (middle). Aerosol extinctions are averaged over the region from  $20^\circ \text{S}$  to  $30^\circ \text{N}$  and from  $5$  to  $105^\circ \text{E}$ . White and gray colors denote periods with no aerosol and no available data, respectively. The black line in the top and middle plots represents the tropopause height as simulated by the model. We sampled aerosol extinction of the model along CALIOP tracks and we averaged them for the region defined before. The bottom plot compares monthly mean AOD for CALIOP (black) and the model (red).

Title Page

Abstract

Introduction

Conclusions

References

Tables

Figures

◀

▶

◀

▶

Back

Close

Full Screen / Esc

Printer-friendly Version

Interactive Discussion



**A permanent aerosol layer in the TTL**

Q. Bourgeois et al.

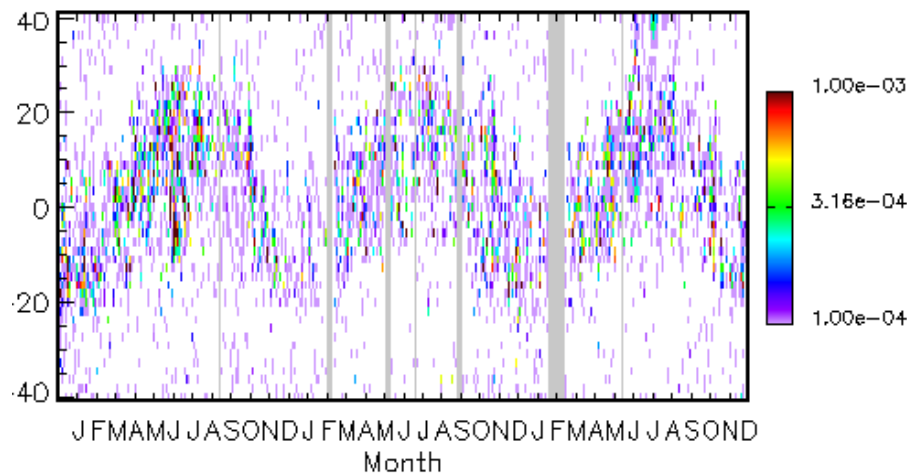


**Fig. 2.** Timeserie of aerosol extinction in the upper troposphere (15 to 20 km) versus latitude for the CALIOP instrument. These data are for a longitude between 5 and 105° E. No-aerosol and no-available-data periods are shown in white and gray, respectively.

[Title Page](#)[Abstract](#)[Introduction](#)[Conclusions](#)[References](#)[Tables](#)[Figures](#)[I◀](#)[▶I](#)[◀](#)[▶](#)[Back](#)[Close](#)[Full Screen / Esc](#)[Printer-friendly Version](#)[Interactive Discussion](#)

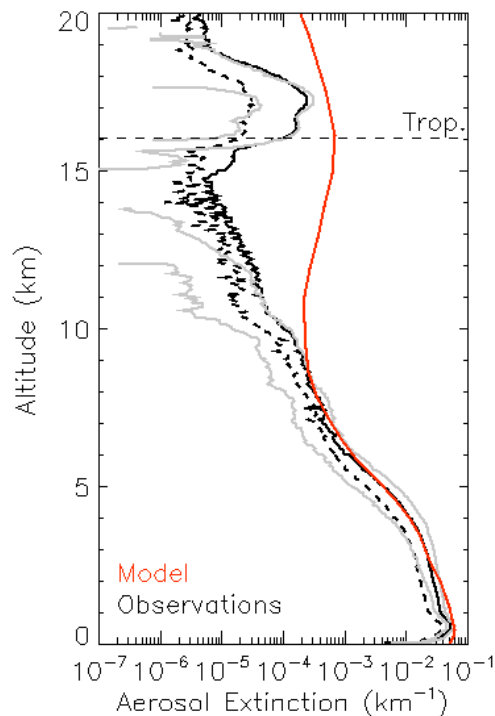


**Fig. 3.** Annual vertical distribution of aerosol extinctions over the Asian region (same as Fig. 1). Observations and model results are in black and red, respectively. The 25–75 % percentiles corresponding to observations are in gray. In the dashed curve, we removed aerosol extinctions having a depolarization ratio larger than 0.05 (see discussion in Sect. 3). The horizontal dashed line represents the tropopause height as simulated by the model.

**A permanent aerosol layer in the TTL**

Q. Bourgeois et al.

Title Page	
Abstract	Introduction
Conclusions	References
Tables	Figures
◀	▶
◀	▶
Back	Close
Full Screen / Esc	
Printer-friendly Version	
Interactive Discussion	



**A permanent aerosol layer in the TTL**

Q. Bourgeois et al.

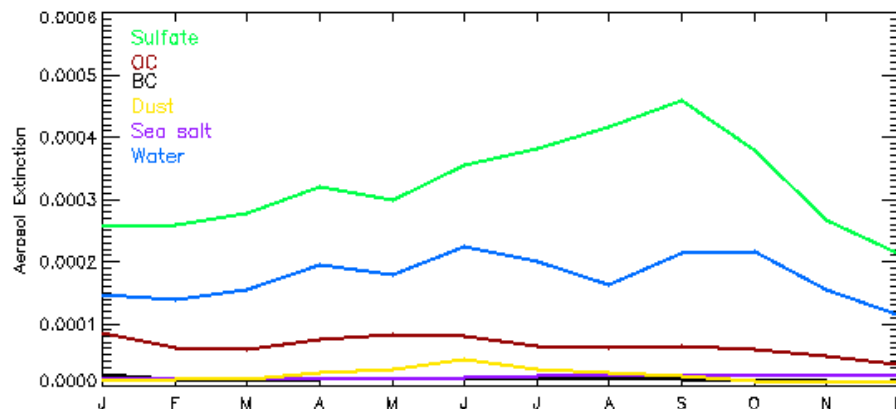


**Fig. 4.** Monthly mean aerosol extinction ( $\text{km}^{-1}$ ) of the aerosol layer (i.e. between 16 and 17 km) over the Asian region (same as Fig. 1) for the different aerosol species simulated by the model.

[Title Page](#)[Abstract](#)[Introduction](#)[Conclusions](#)[References](#)[Tables](#)[Figures](#)[◀](#)[▶](#)[◀](#)[▶](#)[Back](#)[Close](#)[Full Screen / Esc](#)[Printer-friendly Version](#)[Interactive Discussion](#)

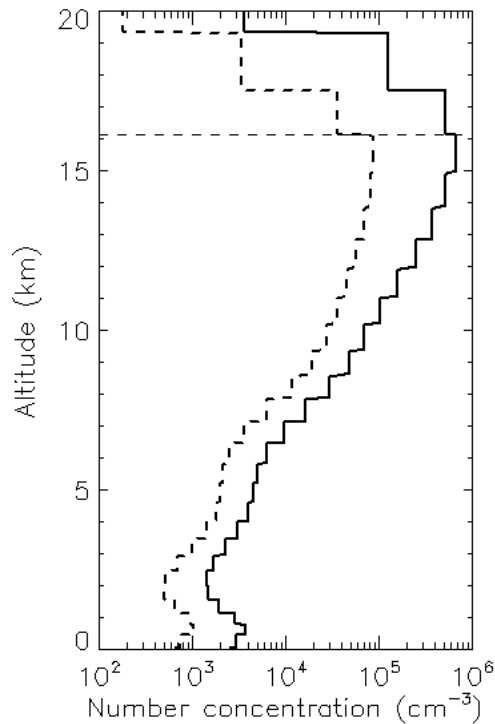


**Fig. 5.** Annual mean vertical profiles of aerosol number concentrations (at STP) in the nucleation mode (black line) and in the nucleation mode with a minimum aerosol size of 3 nm (black dotted line) over the Asian region (same as Fig. 1) for 2007. The horizontal dash line represents the tropopause height as simulated by the model.

**A permanent aerosol layer in the TTL**

Q. Bourgeois et al.

<a href="#">Title Page</a>	
<a href="#">Abstract</a>	<a href="#">Introduction</a>
<a href="#">Conclusions</a>	<a href="#">References</a>
<a href="#">Tables</a>	<a href="#">Figures</a>
<a href="#">◀</a>	<a href="#">▶</a>
<a href="#">◀</a>	<a href="#">▶</a>
<a href="#">Back</a>	<a href="#">Close</a>
<a href="#">Full Screen / Esc</a>	
<a href="#">Printer-friendly Version</a>	
<a href="#">Interactive Discussion</a>	



**A permanent aerosol layer in the TTL**

Q. Bourgeois et al.

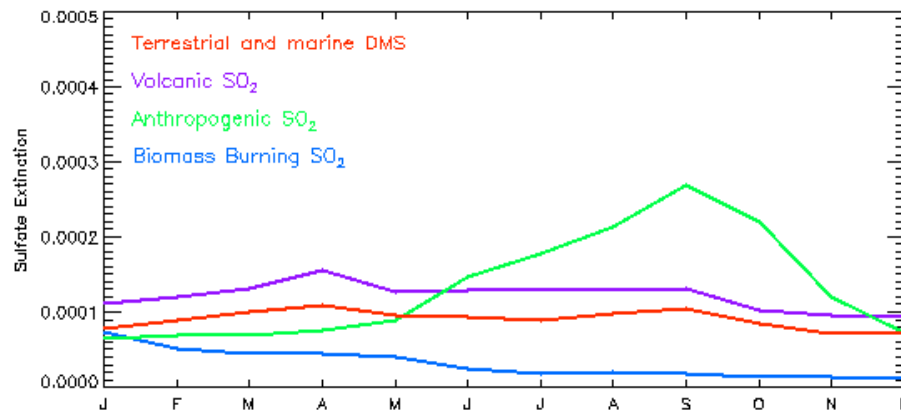


**Fig. 6.** Monthly mean extinction ( $\text{km}^{-1}$ ) in the aerosol layer (same as Fig. 1) for sulfate aerosols resulting from different emission types. These contributions were obtained by subtracting simulations without these emissions from the standard simulation.

[Title Page](#)[Abstract](#)[Introduction](#)[Conclusions](#)[References](#)[Tables](#)[Figures](#)[◀](#)[▶](#)[◀](#)[▶](#)[Back](#)[Close](#)[Full Screen / Esc](#)[Printer-friendly Version](#)[Interactive Discussion](#)

**A permanent aerosol layer in the TTL**

Q. Bourgeois et al.

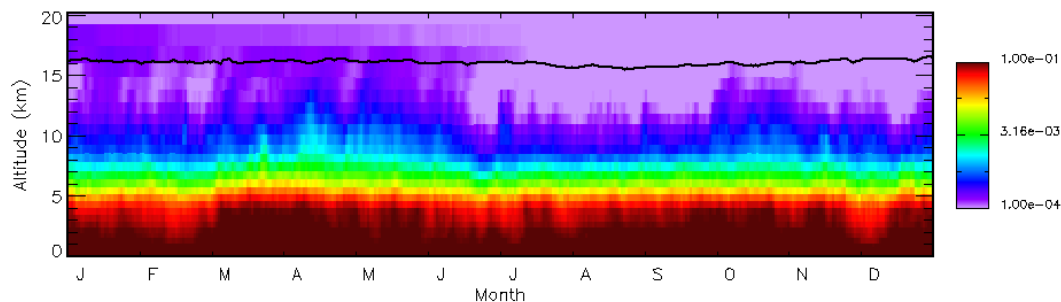


**Fig. 7.** Daily mean vertical aerosol extinctions ( $\text{km}^{-1}$ ) over the Asian region (same as Fig. 1) for 2007 in which we turned off convective transport for all tracers. The black line represents the tropopause height as simulated by the model.

[Title Page](#)[Abstract](#)[Introduction](#)[Conclusions](#)[References](#)[Tables](#)[Figures](#)[◀](#)[▶](#)[◀](#)[▶](#)[Back](#)[Close](#)[Full Screen / Esc](#)[Printer-friendly Version](#)[Interactive Discussion](#)